Terahertz Near-Field Microscope

Kiwon Moon, Euna Jung, Meehyun Lim, Youngwoong Do, and Haewook Han
Department of Electrical Engineering, POSTECH, Pohang, Korea

Abstract

We present a self-consistent line dipole image method for the quantitative analysis of the THz near-field interaction. The line scan across a gold film demonstrated that the terahertz miscroscope has a nanoscale resolution of ~80 nm. The measurements of scattering signals on gold and silicon substrates were in good agreement with calculations.

Keywords : Terahertz Near-Field Microscope

1. Introduction

Conventional THz time-domain spectroscopy (TDS) can provide macroscopic imaging averaged over an ensemble of such nanostructures, which inevitably suffers from inhomogeneous spectral broadening. Moreover, its spatial resolution is limited to ~λ/2 by diffraction. However, nanoscale near-field imaging in the terahertz (THz) spectral range will provide a powerful means for studying intriguing phenomena such as intermolecular vibrational spectroscopy and dynamic charge transport in a variety of quantum-confined nanostructures. Therefore, several types of THz pulse scanning near-field optical microscopes (SNOMs) have been developed to achieve sub-wavelength resolutions [1]-[8]. In this work, we analyze the THz scattering signals of a THz pulse s-SNOM by using a self-consistent line dipole image method (LDIM). We also present a line scan across the edge of a gold film on a GaAs substrate, showing that the THz s-SNOM has a nanoscale resolution of ~ 80 nm. The measurements of the THz scattering signals on gold and GaAs surfaces were in reasonably good agreement with the LDIM calculations [9].

2. Theory and Measurements

The schematic of a THz s-SNOM is shown in Fig. 1 where the incident THz pulse (E_{in}) induces dipole moments in both the probe and the substrate, and the probe is strongly coupled with the substrate, generating the scattered THz pulse (E_{sc}). In general, the analytic theory for the near-field interaction in the probe-substrate system is very involved because the electromagnetic boundary conditions should be matched at the surfaces of the probe and the substrate. Moreover, numerical simulations are practically impossible since the metallic probes requires large mesh sizes and the numerical accuracies are usually not good enough for quantitative comparison with experiments.

In the THz s-SNOM system, the AFM tip oscillates at the mechanical resonance frequency Ω of a quartz tuning fork. The tip-sample gap distance is then given by

$$g(t) = g_0 + g_1(V)\cos\Omega t \tag{1}$$

where t denotes the time coordinate for the tip oscillation, and the oscillation amplitude g_1 is a function of the excitation voltage V applied to the tuning fork. When scanning the time delay of the THz TDS system, the scattered field Esc was measured in the far-field region. Since the near field is a highly nonlinear function of g(t), the scattered field can be expressed as

$$\mathbf{E}_{sc}(t) = \mathbf{E}_0 + \sum_{m=1}^{\infty} \mathbf{E}_m \cos(m\Omega t) \tag{2}$$

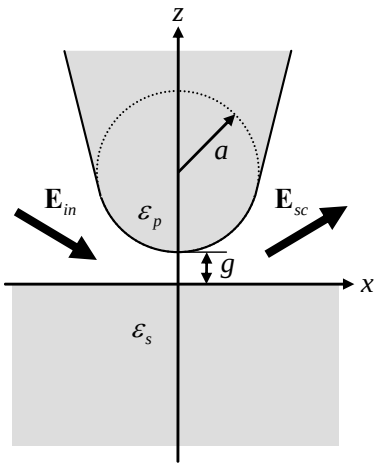

Figure 1: Schematic diagram of a probe-substrate system in THz s-SNOM. The incident field Ein is p-polarized, and the scattered field Esc is measured in the far-field region. In the image analysis, the probe is replaced by a polarizable dielectric sphere.

The large background signal E_0 was suppressed by a lock-in demodulation technique to extract harmonic component E_m. For the analysis and measurement of the near-field interaction, a precise regulation of the oscillation amplitude is essential.

In the pont dipole image method (PDIM), the continuous dipole distributions are usually replaced by point image dipoles. This point-dipole approximation, however, works well only for a large tip-substrate distance. In principle, the electric field from the substrate dipole induces not only a single point dipole but also a continuous dipole distribution in the probe sphere, as we shall see in the line dipole image method (LDIM). In contrast to the PDIM, the LDIM applies exact electrostatic boundary conditions to all dielectric surfaces of the sphere-substrate system through iteration processes, which results in continuous line image dipole densities. This means that the LDIM is self-consistent within the frame work of the polarizable sphere model. Here we describe the LDIM and then present quantitative analyses for the THz near-field interaction in the probe-substrate system.

In the first iteration, the initial dipole moment at the probe sphere is induced by the incident field, resulting in the probe dipole given by

$$\mathbf{d}_{p(1)}^{LD} = \alpha(1+r)\mathbf{E}_{in} \tag{3}$$

where we include the reflection coefficient r at the substrate surface because the actual excitation field is the sum of the incident and reflected fields. It should be noted that we have to consider an image dipole of the radiation source for the incident field to match the exact boundary conditions at the substrate surface. The probe dipole in turn induces the substrate image dipole at $z = -h$ given as

$$\mathbf{d}_{s(1)}^{LD} = \boldsymbol{\beta}_T \cdot \mathbf{d}_{p(1)}^{LD} \tag{4}$$

In the second iteration, the substrate point dipole ds(1)LD induces a line dipole density $\mathbf{p}_{s(2)}{}^{\mathrm{LD}}(z, h) = \gamma(z, h, 2h)\cdot\mathbf{d}_{s(1)}{}^{\mathrm{LD}}$. From the exact image theory, we can derive the substrate-probe image generation dyadic defined as

$$\begin{aligned}\boldsymbol{\gamma}(z,h,L) = {} & \frac{\varepsilon_p - 1}{\varepsilon_p + 1}\left(\frac{a}{L}\right)^3 \delta(z-h+z_K)(\mathbf{I} - 2\mathbf{u}_x\mathbf{u}_x) \\ & + \frac{\varepsilon_p - 1}{(\varepsilon_p+1)^2}\frac{a}{L^2}\left(\frac{h-z}{z_K}\right)^{\frac{1}{\varepsilon_p+1}} [U(z-h+z_K) - U(z-h)][\mathbf{I} + (\varepsilon_p - 1)\mathbf{u}_z\mathbf{u}_z]\end{aligned} \tag{5}$$

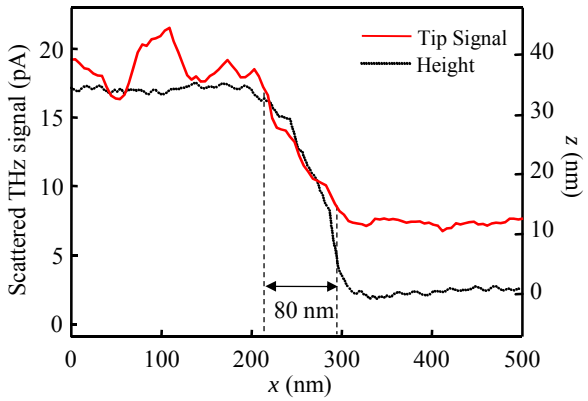

Figure 2: Line scan across the edge of a gold film on a GaAs substrate. The red and black lines represent the THz scattering signal and the AFM topography, respectively. The 10%-to-90% resolution of the THz s-SNOM was ~80 nm.

where $z_K = a^2/L$ is the Kelvin distance, and $\delta(z)$ and $U(z)$ are the Dirac delta and Heaviside unit step functions, respectively. From the third iteration, we must consider not only the point image dipoles but also the line image dipole densities in both the probe and the substrate. For the n^{th} iteration, the probe ($n \geq 3$) and substrate ($n \geq 2$) dipole densities are given by convolution integrals.

$$\begin{aligned} \mathbf{p}^{LD}_{p(n)}(z,h) &= \int_{-h}^{a-h} dz' \boldsymbol{\gamma}(z,h,h-z') \cdot \mathbf{p}^{LD}_{s(n-1)}(z',h) \\ \mathbf{p}^{LD}_{s(n)}(z,h) &= \boldsymbol{\beta}_T \cdot \mathbf{p}^{LD}_{p(n-1)}(-z,h) \end{aligned} \tag{6}$$

and the total dipole moment in the sphere-substrate system is then given by

$$\mathbf{d}^{LD}(h) = \sum_{n=1}^{\infty} \left[\int_{h-a}^{h} dz\, \mathbf{p}^{LD}_{p(n)}(z,h) + \int_{-h}^{a-h} dz\, \mathbf{p}^{LD}_{s(n)}(z,h) \right] \tag{7}$$

Three-dimensional FEM simulations using a commercial software (HFSS) were in excellent agreement with the LDIM calculations on gold and Si substrates.

The samples for the THz line scan were prepared by evaporating a 35 nm thick gold film on the half surface of a semi-insulating GaAs substrate. The etched tip radius of a tungsten wire was a ~ 20 nm. The probe tip was mounted to a quartz tuning fork such that the tip oscillates perpendicularly to the sample surface. As the tip approaches the sample surface, the amplitude, phase, and resonant frequency of the tuning fork's oscillation change. In our experiments, the amplitude was used as a feedback signal for tip-to-sample distance regulation, maintaining a constant tip-substrate distance by controlling the piezo actuator. The incident THz pulses were p-polarized and focused upon an AFM tip with an incident angle of 60º. The THz scattering signal was detected by a THz photoconductive antenna in the far-field region, and simultaneously the AFM topography of the sample surface was obtained from the feedback signals for the piezo actuators of the nanostages.

The THz line scans across the edge of the gold film is shown in Fig. 2, where the first harmonic components (E_1) of the THz scattering signals were used. During the measurements, an oscillation amplitude of g_1 = 45 nm was maintained by a proportional-integral-derivative (PID) controller, and the mechanical delay line was fixed at the positive peaks of the THz scattering pulses. The minimum tip-to-sample distance was less than 1 nm, which is the typical operation condition for our AFM system. The measured tip signal from the Au surface was stronger than that from the GaAs surface as expected from the image theory since the vertical dipole on a metallic surface is enhanced by the image dipole. The THz scattering signal is proportional to the total dipole moment induced in the tip-substrate system, and a metal surface induces larger dipoles than a dielectric surface. The spatial resolution of the THz s-SNOM was ~80 nm, estimated from the 10%-to-90% transition distance in the line scan. The measured scattering field ratio (E1,Au/E1,GaAs)

was 2.5 ± 0.3 which is in good agreement with the calculated scattering ratio of ~2.23, corresponding to the saturation value of scattering ratio for large oscillation amplitude (45 nm) and small tip-sample distance (≤ 1 nm) used in our measurements.

3. Conclusion

The scattering signals in THz pulse s-SNOMs were analyzed by using the line dipole image method. The THz s-SNOM has a nanoscale resolution of ~80 nm. We demonstrated that the relative ratios of the scattering signals measured on gold and GaAs substrates were in good agreement with calculations by the line dipole image theory.

References

[1] S. Hunsche, M. Koch, I. Brener and M.C. Nuss, "THz near-field imaging," *Opt. Comm.*, vol. 150, pp. 22-26, 1998.

[2] N. C. J. van der Valk and P. C. M. Planken, "Electro-optic detection of subwavelength terahertz spot sizes in the near field of a metal tip," *Appl. Phys. Lett.*, vol. 81, no. 9, pp. 1558-1560 ,2002.

[3] T. Yuan, H. Park, J. Xu, H. Han, and X.-C.Zhang, "Field Induced THz Wave Emission with Nanometer Resolution," *Proc. SPIE*, vol. 5649, pp. 1-8, 2005.

[4] H. T. Chen, R. Kersting and G. C. Cho, "Terahertz imaging with nanometer resolution," *Appl. Phys. Lett.*, vol. 83, no. 15, pp. 3009-3011, 2003.

[5] H. Park, J. Kim, and H. Han, "THz Pulse Near-Field Microscope with Nanometer Resolution," presented at the 35th Workshop : Physics and Technology of THz Photonics 2005, Erice, Italy, 20-26 Jul. 2005.

[6] H. Park, J. Kim, M. Kim, H. Han, and I. Park, "Terahertz near-field microscope," presented at the Joint 31st International Conference on Infrared Millimeter Waves and 14th International Conference on Terahertz Electronics (IRMMW-THz 2006), Shanghai, China, 18-22 Sep. 2006.

[7] A. J. Huber, F. Keilmann, J. Wittborn, J. Aizpurua and R. Hillenbrand, "Terahertz Near-Field Nanoscopy of Mobile Carriers in Single Semiconductor Nanodevices," *Nano. Lett.*, vol. 8, no. 11, pp. 3766-3770, 2008.

[8] A. J. Huber, F. Keilmann, J. Wittborn, J. Aizpurua and R. Hillenbrand, "Terahertz Near-Field Nanoscopy of Mobile Carriers in Single Semiconductor Nanodevices," *Nano. Lett.*, vol. 8, no. 11, pp. 3766-3770, 2008.

[9] K. Moon, E. Jung, M. Lim, Y. Do, and H. Han, "Quantitative analysis and measurements of near-field interactions in terahertz microscopes," Opt. Express, vol. 19, no. 12, pp. 11539-11544, 2011.

Acknowledgments

This This work was supported by the National Research Laboratory Program (R0A-2005-001-10252-0), by Basic Science Research Program (2009-0083512), and by Priority Research Centers Program through the National Research Foundation of Korea (NRF) funded by the Ministry of Education, Science and Technology (2010-0029711) and by the Brain Korea 21 Project in 2011.